encit 2020

ABCM Associação Brasileira de Engenharia e Ciências Mecânicas

18th Brazilian Congress of Thermal Sciences and Engineering
November 16–20, 2020 (Online)

ENC-2020-0515
CFD ANALYSIS OF THE WATER/ALUMINA NANOFLUID AS A NUCLEAR REACTOR COOLANT

Luiz Carlos Aldeia Machado
Nuclear Engineering Department, Federal University of Rio de Janeiro - POLI/UFRJ
aldeia@poli.ufrj.br

Carolina da Silva Bourdot Dutra
Nuclear Engineering Department, Federal University of Rio de Janeiro - POLI/UFRJ
cdutra@poli.ufrj.br

Gabriel Caetano Gomes Ribeiro da Silva
Nuclear Engineering Program, Federal University of Rio de Janeiro - COPPE/UFRJ
gcsilva@nuclear.ufrj.br

Abstract. *The arising demand for reliable and clean energy sources emphasizes the need to optimize nuclear reactors. In this context, the enhancement of the coolant heat transfer provided by nanofluids has been investigated by an increasing number of researchers. The objective of this work is the analysis of the steady-state thermal-hydraulic behavior of the water/alumina nanofluid as a coolant in a square arrayed rod bundle subchannels of a PWR with pitch-to-diameter ratios of 1.1, 1.2, and 1.3 and nanoparticle concentrations (φ) ranging from 0 to 4.5%. The Reynolds number (Re) was varied from 3×10^5 to 6×10^5. The mathematical model was composed of the Reynolds-averaged Navier-Stokes equations (RANS) and the standard k-ϵ turbulence model, solved using the commercial Computational Fluid Dynamics (CFD) tool, ANSYS Fluent v19.2. First, the geometric models and the meshes were created and a mesh sensitivity study was performed. The results were successfully verified through the comparison with correlations from the literature. The Nusselt number was found to increase with Re and φ, while the friction factor decreased with Re and increased with φ. A correlation was proposed for the Nusselt number, valid for a wider range of parameters, compared to the existing correlations. It was concluded that higher values of Re and φ as well as lower values of P/D provide a more efficient heat transfer considering the trade-off between heat transfer enhancement and pressure drop increment.*

Keywords: *CFD, nanofluid, thermal-hydraulics, nuclear reactor*

1. INTRODUCTION

In order to meet the world's increasing demand for energy, it is necessary to optimize the current power generation systems. In nuclear reactors, the enhancement of the coolant heat transfer rate is essential to decrease the design scale and the operational costs. Recently, the use of nanofluids as high-performance coolants has been investigated by an increasing number of researchers. The presence of dispersed nanoparticles in a base fluid, such as water, can boost the overall heat removal as the resulting mixture, called nanofluid, presents a substantially higher thermal conductivity when compared to the pure base fluids. The dispersion of nanoparticles within a nuclear reactor coolant may ultimately enable the reactor to operate at a higher power level, leading to economic gains and higher safety margins.

Several experimental and numerical works have been conducted with different nanofluid mixtures. Among the most common are water and ethylene glycol as base fluids, with metallic nanoparticles, such as copper, titanium, or aluminum — due to their high thermal conductivity.

Primary studies of nanofluids in nuclear reactors carried out by Buongiorno *et al.* (2008) reported that the use of nanoparticles rendered up to a 20%-power-density increase in the reactor core. Additionally, the presence of nanoparticles did not change significantly the core neutronic behavior and the alumina nanofluid presented an acceptable coolant radioactivity level during the shutdown, proving their suitability as nuclear reactor coolants.

The adequate modeling of nanofluids thermophysical properties is a key parameter towards achieving accurate results. For Al_2O_3 (alumina), TiO_2 and CuO nanofluids, with volumetric concentrations ranging from 1 to 5%, it was observed that the fuel rod heat removal capacity was enhanced. However, it was accompanied by a significant increase in the pressure drop due to the higher viscosity of nanofluids (Bafrani *et al.*, 2020).

The nanofluid properties can be implemented by considering one of the two following models: a single-phase ho-

mogeneous mixture or a two-phase mixture — assuming that nanoparticles flow in a distinct phase. Through the CFD modeling of the water-Al_2O_3 nanofluid flow in a triangular array reactor, Hadad *et al.* (2013) concluded that the two-phase model was more accurate for small concentrations of nanoparticles, though when the concentration was as big as 0.05%, the difference between the two models got smaller.

The thermal-hydraulic analysis of the alumina nanofluid carried out by Zafiri *et al.* (2013), Zarifi and Tashakor (2015), and Osman *et al.* (2019) indicated that the deviation between water and alumina nanofluid heat transfer coefficients at low nanoparticle volume percentage was negligible, and significant changes only occurred at volume percentage values above 1.0%.

Shamim *et al.* (2016) studied the water/alumina nanofluid single-phase flow in a square array reactor subchannel for high Reynolds numbers using the pitch-to-diameter ratios (P/D) of 1.25 and 1.35 and compared the results with the correlations found in the literature. They also concluded that the convective heat transfer coefficient was enhanced with the increase of nanoparticle concentration, and the traditional correlations for heat transfer in subchannels, such as the Presser correlation, were unable to predict the Nusselt number under those conditions.

Considering the trade-off between heat transfer enhancement and pressure drop increment, and the lack of correlations in the literature, it becomes necessary to further investigate the thermal-hydraulics of nanofluids in nuclear reactors subchannels, considering the effect of the most commonly affecting parameters, such as the pitch-to-diameter ratio and the nanofluid volume fraction.

This work presents the Computational Fluid Dynamics (CFD) analysis of a water/alumina nanofluid coolant flowing in a pressurized water reactor (PWR) subchannel. Three square arrayed subchannels with pitch-to-diameter ratios of 1.1, 1.2, and 1.3 were modeled to analyze the coolant flow with nanoparticle volume concentrations ranging from 0 to 4.5%, and Reynolds number varying from 300,000 to 600,000.

2. METHODOLOGY

The physical model consists of three different subchannel geometries, corresponding to three values of P/D (1.1, 1.2, and 1.3). The diameter of the fuel rod D was kept constant, while the pitch P varied from one geometry to another. In order to decrease the computational cost, only 1/8 of a centralized fluid cell was modeled, considering the widely utilized hypothesis that subchannels present axisymmetric flows, for most fluids, under forced convection (Hooper, 1980). Figure 1 illustrates the geometry, with 1/8 of the subchannel hatched.

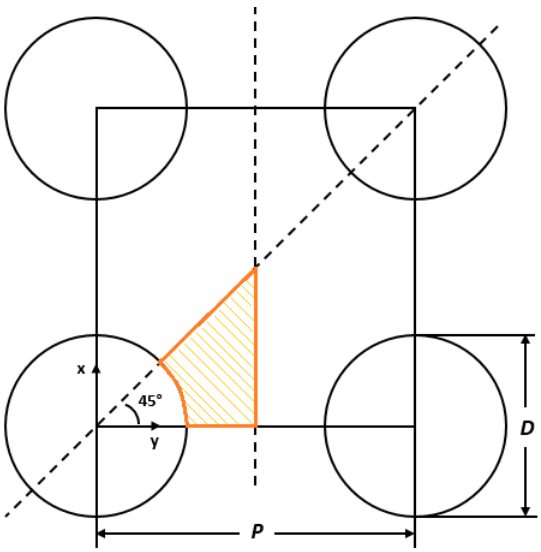

Figure 1: Cross sectional representation of the subchannel.

For the nanofluid flow in the subchannel, the following boundary conditions were assumed:

- specified temperature, pressure, and mass flow rate at the inlet;
- uniform velocity at the inlet;
- zero velocity at the solid surface (fuel rod wall);
- symmetry condition at the side faces of the channel;
- cosine heat flux at the fuel rod wall.

The cosine heat flux ($q''(z)$) imposed is expressed by:

$$q''(z) = \frac{q'_0}{\pi D} cos\left(\frac{\pi z}{L}\right) \tag{1}$$

where L is the subchannel length, z is the axial position and q'_0 is a constant, representing the maximum linear heat generation rate of a fuel rod. The geometric parameters and conditions assumed are based on a PWR (Tab. 1).

Table 1: Geometric parameters and conditions of the model.

Name	**Symbol**	**Value**
Fuel rod diameter	D	9.50 mm
Subchannel length	L	3.66 m
Maximum linear heat generation rate	q'_0	17.80 kW/m
Pitch	P	10.45 mm, 11.40 mm, 12.35 mm
Pressure	p	15.0 MPa
Inlet temperature	T_{in}	559.15 K

The nanofluid consists of Al_2O_3 nanoparticles dispersed in water. Four values of nanoparticle volume concentrations (φ) were considered: 0.0, 1.5, 3.0, and 4.5%. The Reynolds numbers ranged from 3.0×10^5 to 6.0×10^5, with increments of 10^5.

The mathematical model, considering the steady-state assumption, is composed by the following conservation equations:

Continuity equation:

$$\bigtriangledown \cdot (\rho \vec{u}) = 0, \tag{2}$$

where ρ is the density and u is velocity (m/s).

Momentum equation:

$$\bigtriangledown \cdot (\rho u \vec{u}) = - \bigtriangledown p + \bigtriangledown \cdot \vec{\vec{\tau}} + \rho \vec{g}, \tag{3}$$

where g is the acceleration of gravity, p is the pressure and τ is the stress tensor.

Energy equation:

$$\bigtriangledown \cdot (\rho \vec{u} e) = \bigtriangledown \cdot (k \bigtriangledown T) - p \bigtriangledown \vec{u}, \tag{4}$$

where k is the thermal conductivity, e is the internal energy and T is the temperature.

The turbulence model chosen was standard k-ϵ, due to its faster convergence and elevated robustness. Additionally, a standard wall function was used to enhance the fluid resolution within the boundary layer (Launder and Spalding, 1974). The transport equations were discretized using the Finite Volumes Method implemented by the commercial CFD software, ANSYS-Fluent v.19.2.

The nanofluid was assumed to be a single-phase homogeneous mixture. The fluid properties were implemented as variable with temperature (fifth degree polynomials) and were calculated based on the data from NIST REFPROP v.7, for pure water, and the following expressions, used by Bianco *et al.* (2009) and Shamim *et al.* (2016):

$$\rho_{nf} = (1 - \varphi)\rho_{bf} + \varphi \rho_{np} \tag{5}$$

$$C_{p_{nf}} = (1 - \varphi) C_{Pbf} + \varphi C_{p_{np}} \tag{6}$$

$$\mu_{nf} = (1 + 7.3\varphi + 123\varphi^2)\mu_{bf} \tag{7}$$

$$k_{nf} = (1 + 2.72\varphi + 4.97\varphi^2)k_{bf} \tag{8}$$

where ρ, C_p and μ and k stand for density, specific heat, viscosity, and thermal conductivity of the nanofluid, respectively. The subscripts nf, bf and np represent nanofluid, base fluid and nanoparticle, respectively.

For the analysis of the simulation results, the local properties were calculated for each of the 1,000 equally-spaced planes, perpendicular to z, created along the subchannel. The bulk temperature T_b was defined as the mass flow averaged temperature; the wall temperature T_w and the wall heat flux q'', as the average along the intersection between the planes and the fuel rod wall. The pressure p was calculated as an area average. The average velocity v was obtained by:

$$v = \frac{\dot{m}}{\rho A} \tag{9}$$

where $\dot{m}$ is the mass flow rate and A is the area of the subchannel cross-section.

The thermophysical properties were calculated at the bulk temperature at each plane. The local dimensionless numbers considered in this work are the following:

Reynolds number (Re):

$$Re = \frac{v\rho D_h}{\mu} \tag{10}$$

where D_h is the hydraulic diameter of the subchannel, obtained by:

$$D_h = \frac{4P^2 - \pi D^2}{\pi D} \tag{11}$$

Nusselt number (Nu):

$$Nu = \frac{hD_h}{k} \tag{12}$$

with the local heat transfer coefficient h calculated by:

$$h = \frac{q''}{T_b - T_w} \tag{13}$$

Prandtl number (Pr):

$$Pr = \frac{\mu C_p}{k} \tag{14}$$

The Fanning friction factor f was defined as:

$$f = -\frac{D_h}{2\rho v^2}\frac{\Delta p}{\Delta z} \tag{15}$$

The Nusselt number and the friction factor of the subchannel were calculated as the average of the local quantities along the entire subchannel, disregarding the regions at the vicinity of the inlet and the outlet, to ensure the fully developed flow condition. The length of these regions L_d was taken as (Todreas and Kazimi, 1990):

$$L_d = 40 \cdot D_h \tag{16}$$

For the verification of the results, the correlations presented in Tab. 2 were used.

Finally, in order to compare the simulation results with the analytical model, an iterative algorithm was built for calculating simultaneously the mean temperature of the entire subchannel and the C_p at this temperature, using the following equation for the outlet temperature T_{out} (Todreas and Kazimi, 1990):

$$T_{out} = T_{in} + \frac{2q'_0 L}{\pi \dot{m} C_p} \tag{17}$$

Table 2: Correlations used in this work.

Authors	**Correlation**
Dittus-Boelter (Todreas and Kazimi, 1990)	$Nu_{DB} = 0.023Re^{0.8}Pr^{0.4}$
	$Re \geq 10^5$, $0.6 \leq Pr \leq 160$
Presser (Todreas and Kazimi, 1990)	$Nu_{Presser} = Nu_{DB} \cdot (0.9217 + 0.1478P/D - 0.1130e^{-7(P/D-1)})$
	$Re \geq 10^5$, $0.6 \leq Pr \leq 160$, $1.05 \leq P/D \leq 1.90$
Shamim *et al.* (2016)	$Nu = (Nu_{Presser})_{water} \cdot (1 + 0.0247\varphi^{1.39})$
	$3{\times}10^5 \leq Re \leq 6{\times}10^5$, $0.847 \leq Pr \leq 1.011$, $1.25 \leq P/D \leq 1.35$, $0.5\% \leq \varphi \leq 3.0\%$
Cheng and Todreas (1986)	$\frac{1}{4} \cdot (0.1339 + 0.09059(P/D-1) - 0.09926(P/D-1)^2) \cdot Re^{-0.18}$
	$0.847 \leq Pr \leq 1.011$, turbulent Reynolds number

From the evaluated C_p, taken as a constant at the mean temperature, the bulk temperature as a function of z was calculated by:

$$T(z) = T_{in} + \frac{q'_0 L}{\pi \dot{m} C_p}\left(sin\frac{\pi z}{L} + 1\right) \tag{18}$$

3. RESULTS

For the preliminary mesh independence analysis, the case where P/D = 1.1, φ = 0.0% and Re = 600,000 was taken as reference, since this configuration presents the greatest variation of properties and the biggest velocity gradient. Eight unstructured meshes with an increasing number of elements were generated for this case and the analyzed variable was the outlet temperature T_{out}. The results, presented in Fig. 2(a), show that the most refined meshes provide very similar results. The chosen mesh was the second most refined (7^{th} mesh), whose cross-section is presented in Fig. 2(b). For the other geometries, the meshes were made using the same element size and near-wall refinement parameters of the chosen mesh in the reference case.

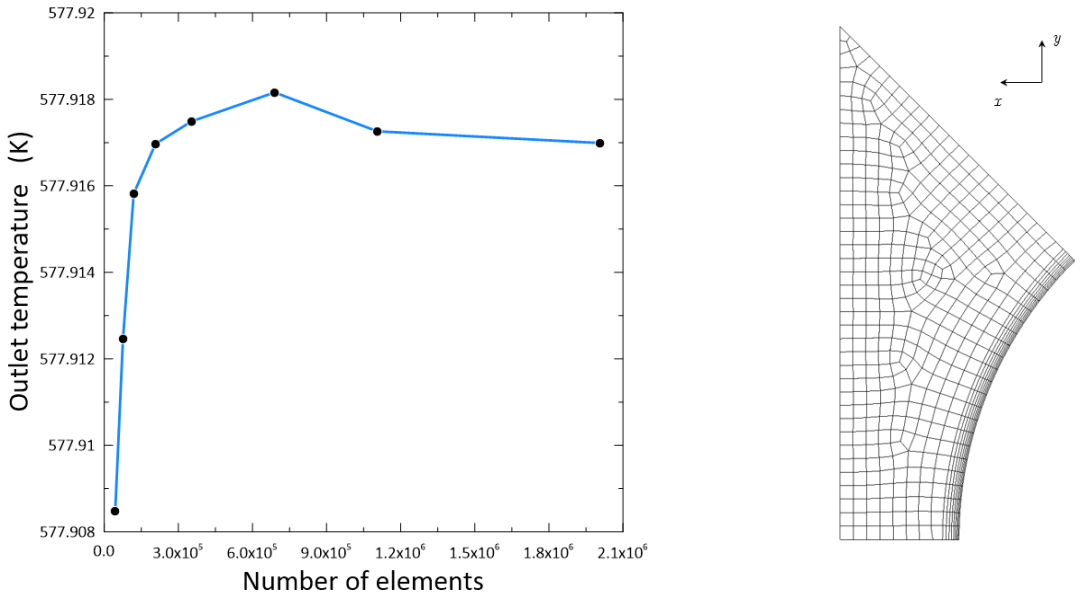

(a) (b)

Figure 2: 2(a) Outlet temperature as a function of the number of mesh elements, 2(b) cross-section of the chosen mesh.

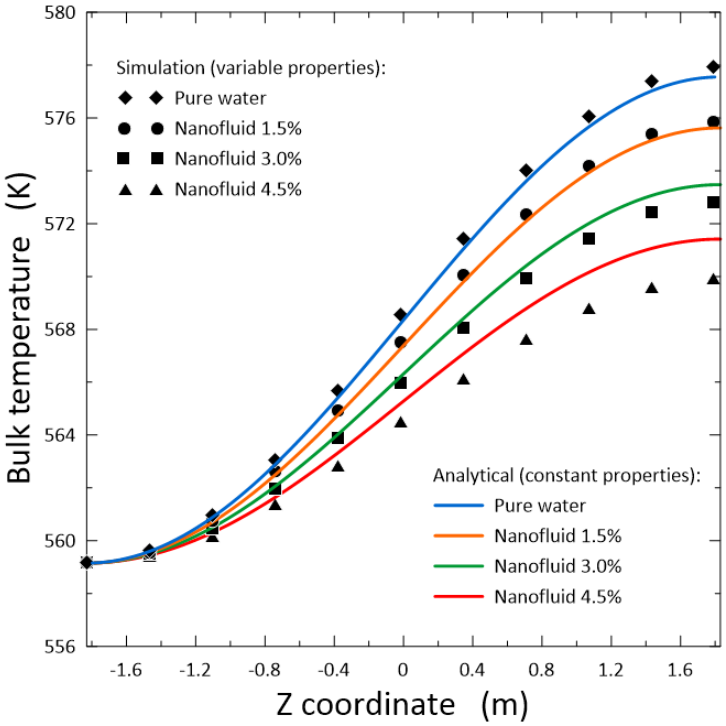

Figure 3: Bulk temperature as a function of the axial coordinate for the simulations and the analytical model (P/D = 1.1).

A comparison of the simulations and the analytical results are presented in Fig. 3, where the bulk temperature T_b was plotted as a function of the axial coordinate z, for the case where P/D = 1.1. It can be observed that the assumption of a constant value for C_p generates inaccuracy (especially when $\varphi \geq 3.0\%$), reinforcing that the variable properties model is the most adequate for this problem. It can also be oberved from the figure that higher values of φ decrease the outlet temperature, wich is in agreement with the conclusions made by Shamim (2015)

The simulation results for the Nusselt number and the friction factor as functions of the Reynolds number, for the cases with P/D = 1.3, are presented in Fig. 4. It can be observed that the Nusselt number increases with Re and φ, while the friction factor decreases with Re and increases at φ. The friction factor has shown to be less affected by the variation of φ than the Nusselt number. The results presented a good agreement with the correlations, with an average deviation of 5.8% for Nu and 6.2% for f.

Considering that the correlation from Shamim *et al.* (2016) is only valid for $1.25 \leq P/D \leq 1.35$ and $0.5 \leq \varphi \leq 3.0$, the following correlation has been proposed for the Nusselt number:

$$Nu = (Nu_{Presser})_{water} \cdot (0.8963 + 0.02547\varphi^{1.61284}) \tag{19}$$

valid for $1.1 \leq P/D \leq 1.3$, $0.0 \leq \varphi \leq 4.5$ and $0.80 \leq Pr \leq 1.37$.

The above correlation was obtained via nonlinear regression using the software Wolfram Mathematica v. 11.3. The method employed was the Levenberg-Marquardt and the obtained coefficient of determination R^2 was 0.992.

Figure 5 shows the relation between the Nusselt numbers obtained from the simulation and the ones calculated by the proposed correlation. The proposed correlation presented an average deviation of 7.7%, whereas the correlation of Shamim *et al.* (2016) presented a 10.4% deviation when compared to the simulation results.

The relation between the Nusselt number calculated by the proposed correlation and the friction factor calculated by the correlation of Cheng and Todreas (1986) is presented in Fig. 6. In this figure, all the curves present a descending behavior. This is due to the increasing Reynolds number — not represented in the figure. Thus, it can be observed that higher values of Re and φ as well as lower values of P/D provide a more efficient heat transfer, which is, a higher heat transfer enhancement for a lower pressure drop increment.

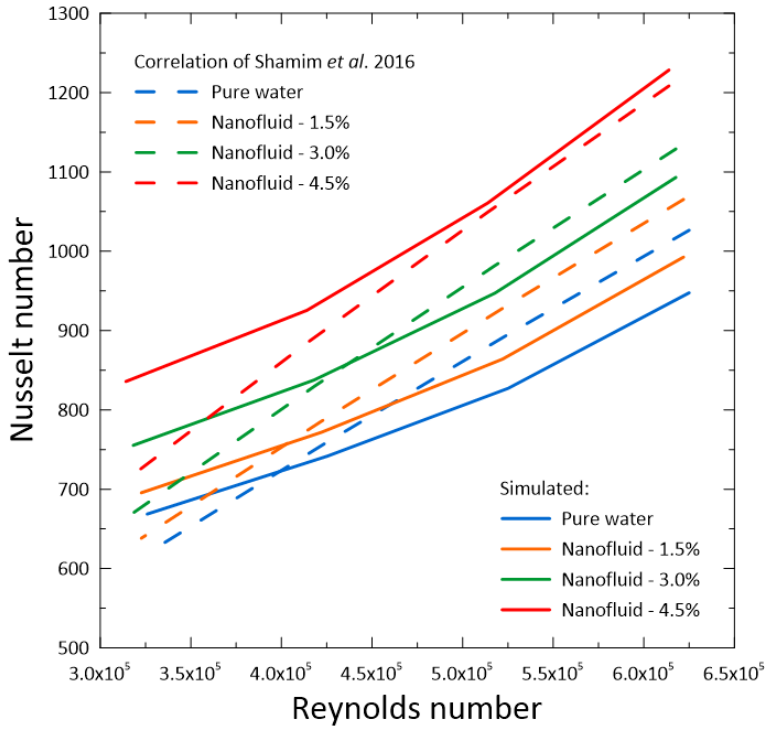

(a)

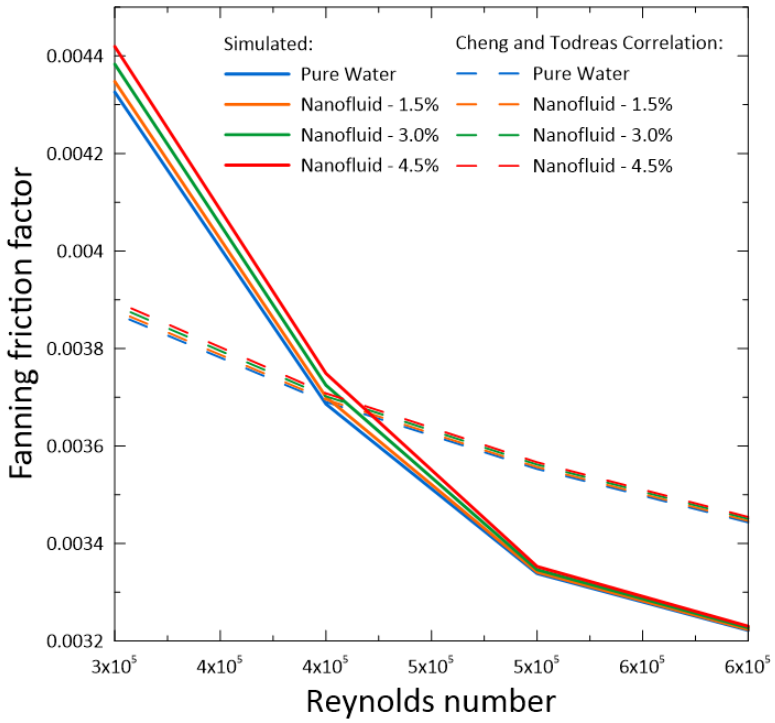

(b)

Figure 4: 4(a) Nusselt number and 4(b) friction factor as functions of the Reynolds number, for P/D = 1.3.

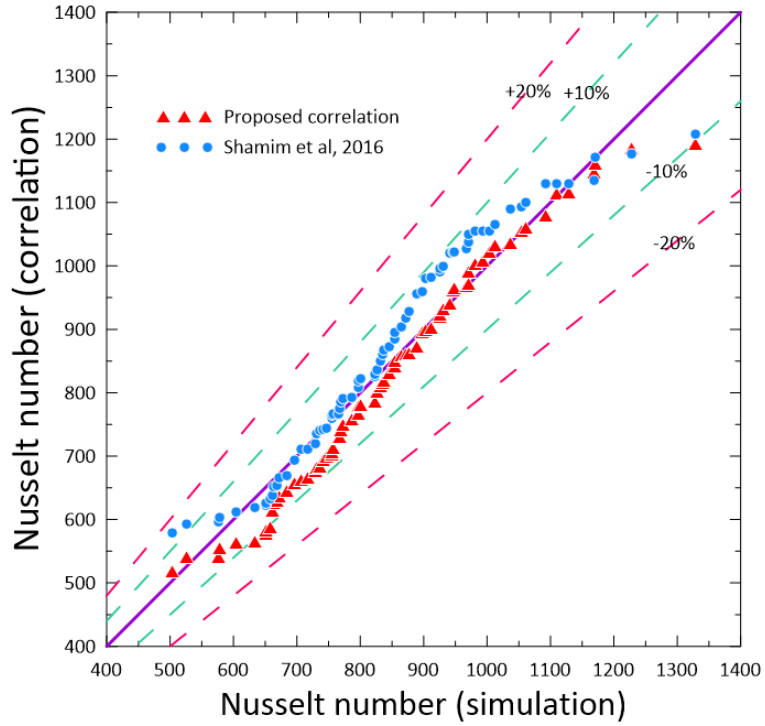

Figure 5: Nusselt number calculated by the proposed correlation as a function of the Nusselt number obtained from the simulations.

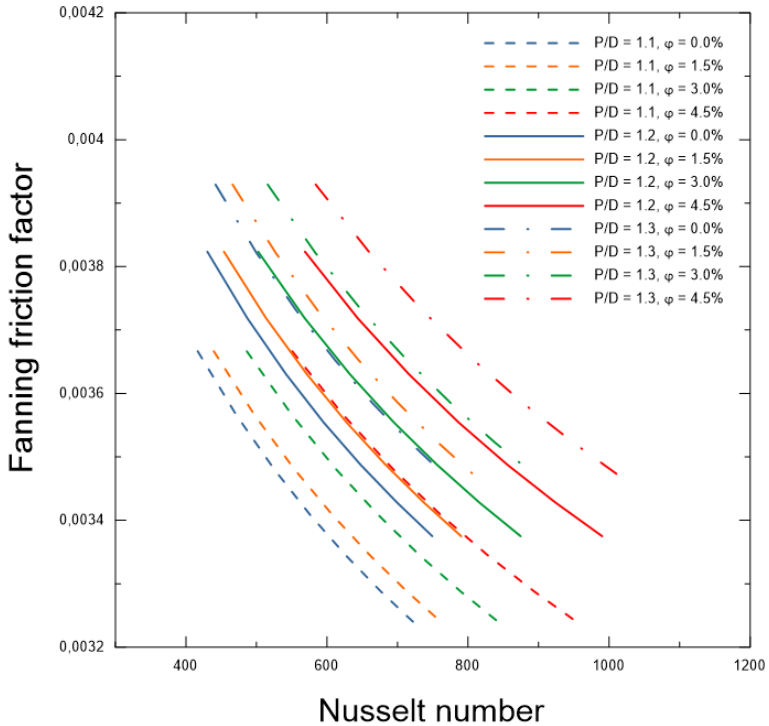

Figure 6: Nusselt number calculated by the proposed correlation as a function of the friction factor calculated by the correlation of Cheng and Todreas (1986).

4. CONCLUSION

The thermal-hydraulics of the nanofluid flow as a coolant in a PWR subchannel was successfully investigated via CFD. The results agreed with the existing correlations in the literature. The following conclusions were taken:

The Nusselt number increases with Re and φ, while the friction factor decreases with Re and increases with φ;

The correlation of Shamim *et al.* (2016) for the Nusselt number presented a good agreement with the results for P/D = 1.3 — with a 5.8% average deviation —, but it was not valid for the other values of P/D studied. The correlation of Cheng and Todreas (1986) for the friction factor also agreed well with the results — with a 6.2% average deviation, for the case where P/D = 1.3.

A new correlation for the Nusselt number was proposed for a larger range of P/D and φ, and presented an average deviation of 7.7% when compared to all the simulation results. On the other hand, the correlation of Shamim *et al.* (2016) presented a 10.4% average deviation.

Finally, it can be concluded that, for the range of parameters studied, higher values of Re and φ, as well as lower values of P/D, provide a more efficient heat transfer due to the higher values of Nu and the lower values of f.

5. ACKNOWLEDGEMENTS

The authors are grateful to the Brazilian National Council for Scientific and Technological Development (CNPq) for their financial support.

6. REFERENCES

Bafrani, H.A., Noori-kalkhoran, O., Gei, M., Ahangari, R. and Mirzaee, M.M., 2020. "On the use of boundary conditions and thermophysical properties of nanoparticles for application of nanofluids as coolant in nuclear power plants; a numerical study". *Progress in Nuclear Energy*, Vol. 126.

Bianco, V., Chiacchio, F., Manca, O. and Nardini, S., 2009. "Numerical investigation of nanofluids forced convection in circular tubes". *Applied Thermal Engineering*, Vol. 29, p. 3632–3642.

Buongiorno, J., Hu, L.W., Kim, S.J., Hannink, R., Truong, B. and Forrest, E., 2008. "Nanofluids for enhanced economics and safety of nuclear reactors: an evaluation of the potential features, issues, and research gaps". *Nuclear Technology*, Vol. 162, pp. 80–91.

Cheng, S.K. and Todreas, N.E., 1986. "Hydrodynamic models and correlations for bare and wire-wrapped hexagonal rod bundles — bundle friction factors, subchannel friction factors and mixing parameters". *Nuclear Engineering and Design*, Vol. 92, No. 2, pp. 227 – 251.

Hadad, K., Rahimian, A. and Nematollahi, M.R., 2013. "Numerical study of single and two-phase models of water/Al2O3 nanofluid turbulent forced convection flow in VVER-1000 nuclear reactor". *Annals of Nuclear Energy*, Vol. 60, pp. 287–294.

Hooper, J.D., 1980. "Developed single phase turbulent flow through a squared-pitch rod cluster". *Nuclear Engineering and Design*, Vol. 60, pp. 365–379.

Launder, B.E. and Spalding, D.B., 1974. "The numerical computation of turbulent flows". *Computer Methods in Applied Mechanics and Engineering*, Vol. 3, pp. 269–289.

Osman, S., Sharifpur, M. and Meyer, J.P., 2019. "Experimental investigation of convection heat transfer in the transition flow regime of aluminium oxide-water nanofluids in a rectangular channel". *International Journal of Heat and Mass Transfer*, Vol. 133, pp. 895–902.

Shamim, J.A., Bhowmik, P.K., Xiangyi, C. and Suh, K.Y., 2016. "A new correlation for convective heat transfer coefficient of water–alumina nanofluid in a square array subchannel under pwr condition". *Nuclear Engineering and Design*, Vol. 308, pp. 194–204.

Shamim, J.A., 2015. *Numerics Applied Nanofluid Analysis in a Square Array Subchanne*. Master's thesis, Seoul National University.

Todreas, N.E. and Kazimi, M.S., 1990. *Nuclear Systems I*. Taylor & Francis, New York, USA.

Zafiri, E., Jahanfarnia, G. and Veysi, F., 2013. "Subchannel analysis of nanofluids application to VVER-1000 reactor". *Chemical Engineering Research and Design*, Vol. 91, pp. 625–632.

Zarifi, E. and Tashakor, S., 2015. "Subchannel analysis of Al2O3 nanofluid as a coolant in vmhwr". *Kerntechnik*, Vol. 80, pp. 440–448.

7. RESPONSIBILITY NOTICE

The authors are solely responsible for the printed material included in this paper.